Wave chaos in quantized classically nonchaotic systems

P. Šeba*
Institute of Mathematics, Ruhr University Bochum, Bochum, Germany

K. Życzkowski†
Department of Physics, University of Essen, D-4300 Essen 1, Germany
(Received 10 December 1990)

We discuss the properties of the wave chaos appearing in some quantized systems that are classically not chaotic.

I. INTRODUCTION

The question of what extent quantum systems reflect the chaotic behavior present in classical dynamical systems has recently attracted much attention [1–10]. A large number of numerical studies performed on these systems showed that their local statistical spectral properties are well described by random-matrix theory (RMT). This is in sharp contrast with the level statistics for integrable systems, which in the generic case are given by a Poisson distribution.

In addition to the numerical evidence, there are also theoretical studies that support the idea of describing quantized chaotic systems with RMT. This correspondence is, however, limited due to the fact that the quantum system displays a strong influence of classical (unstable) periodic orbits. This leads to such additive structures as scars [6], oscillatory behavior of the spectral rigidity [11], etc., which lie outside of the scope of the RMT description.

The lesson one can draw from the existence of scars is that the role of some individual classical orbits can be enhanced following quantization. In what follows we are concerned with classical systems that contain unstable orbits, which are, however, of measure zero, so that the system is not chaotic from the classical point of view. As a typical example let us mention the billiard plotted in Fig. 1, where orbits hitting the edge of the indicated corner are unstable. After quantization the unstable orbits spread into a finite portion (because of the uncertainty principle), and the system is expected to develop typical chaotic characteristics. In this way *quantization induces chaotic properties to systems that are classically not chaotic.* In order to distinguish this property from quantum chaos (which means quantized *classically chaotic* systems), we will call this phenomenon "wave chaos."

The simplest way to get a wave-chaotic Hamiltonian is to use the correspondence principle and quantize some classical pseudointegrable system (cf. Fig. 1). This procedure leads, however, to complicated operators that can hardly be handled mathematically. Even numerical investigation of these systems is very difficult and the amount of available data is quite limited. Our aim here is to use a different approach and construct the chaotic quantum Hamiltonian directly. What we obtain is a system that displays all the features of well-developed wave chaos, and at the same time is simple enough to be analyzed mathematically.

II. CONSTRUCTION OF THE HAMILTONIAN

Let us consider the Sinai billiard, i.e., a point particle that moves inside a rectangular wall enclosing a circular reflecting obstacle with radius R. Sinai proved [12] that this system is classically fully chaotic for all $R > 0$. The corresponding quantum system has been numerically investigated by Berry [13] and Bohigas, Giannoni, and Schmidt [14], who compared its level statistics with the predictions of RMT and found good overall agreement. Thus the Sinai billiard is a system in which the influence of classical chaos on quantum mechanics has been successfully tested.

The quantized Sinai billiard is, however, too complicated to solve analytically, so one is left with numerical results only. Our aim is therefore to construct a similar but more tractable model on which to pursue the mathematical analysis. Our argument goes as follows: We start with the Sinai billiard and shrink the radius R of the obs-

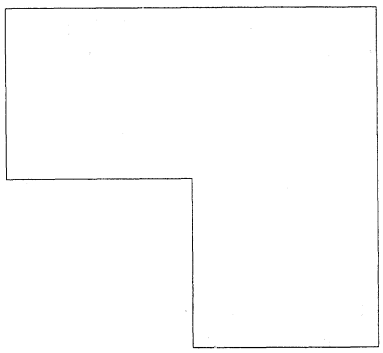

FIG. 1. Example of a pseudointegrable billiard.

tacle to zero, replacing it by a point scatterer [15,16]. In the limiting case the only classical trajectories influenced are those that hit the scattering point; they are hence of measure zero. The system is therefore not chaotic from the classical point of view.

Quantum waves are, however, scattered by the point scatterer. This means that its properties are in some sense similar to those of the original Sinai billiard and that wave chaos is expected to appear.

Let us now pass to the construction of the Hamiltonian H. The difficult point is of course to describe the point scatterer. We will do this by employing the theory of singular interactions developed by Albeverio *et al.* [17] and construct the relevant operator as follows: We start with the Hamiltonian H of the standard rectangular billiard Ω,

$$H=-\Delta ,$$
$$D(H)=\{f\in L^2(\Omega) , p^2\hat{f}(p)\in L^2(\mathbb{R}^2) , \text{ and } f=0 \text{ on } \delta\Omega\} , \tag{1}$$

where

$$\Omega=\left[0;\frac{\pi}{a}\right]\times[0;\pi]$$

is a rectangle with site lengths π/a and π (we will assume a to be an irrational number, i.e., the billiard Ω has incommensurate sites), $\delta\Omega$ denotes the border of the billiard, and $\hat{f}$ is the Fourier transform of f.

We remove now the relevant scattering point $\mathbf{x}_0=(x_0,y_0)\in\Omega$ restricting H to H_0

$$H_0=H|D_0 ,$$
$$D_0=\{f\in D(H),\ f\equiv 0 \text{ in some neighborhood of the point } \mathbf{x}_0\} . \tag{2}$$

The operator H_0 is symmetric but not self-adjoint. In order to obtain a self-adjoint operator we have to specify what happens when the particle hits the removed point $\mathbf{x}_0$. This will be done with the help of the theory of self-adjoint extensions (see [17]). It is not difficult to show that the operator H_0 has deficiency indices (1;1). Hence there exists exactly one one-parameter family of its self-adjoint extensions; the free parameter might be interpreted as the coupling constant. According to Zorbas [18] the deficiency subspaces $\mathcal{H}^{\pm}$ are spanned by the Green's function of the operator H,

$$\mathcal{H}^{\pm}=\{f;f(\mathbf{x})=cG(\mathbf{x};\mathbf{x}_0;\pm i);c\in\mathbb{C}\} , \tag{3}$$

with $G(\mathbf{x},\mathbf{y};z)$ defined as

$$(H-z)^{-1}f(x)=\int_\Omega G(\mathbf{x},\mathbf{y},z)f(\mathbf{y})d^2y . \tag{4}$$

The one-parameter family H_Θ of all self-adjoint extensions of H_0 is then given by the following theorem.

Theorem 1. All self-adjoint extensions H_Θ of the operator H_0 are given by

$$H_\Theta=-\Delta$$
$$D(H_\Theta)=\{f\in L^2(\Omega),f(\mathbf{x})=\varphi(\mathbf{x})+cG(\mathbf{x};\mathbf{x}_0;i) -ce^{i\Theta}G(\mathbf{x};\mathbf{x}_0;-i);\ \varphi\in D_0;\ c\in\mathbb{C};\ \Theta\in[0,2\pi]\} . \tag{5}$$

Our task is to investigate the level-spacing statistics of the operator H_Θ. It is, however, difficult to solve the spectral problem directly because of the abstract definition of the operator. We will therefore use indirect methods and obtain the spectrum of H_Θ by analyzing the pole structure of its resolvent, which is given by Krein's formula [18].

Theorem 2. (Zorbas version of Krein's formula). Let H_Θ; $\Theta\in[0,2\pi)$ be the self-adjoint extension of the operator H_0 described by Theorem 1. Then its resolvent is given as

$$(H_\Theta-z)^{-1}=(H-z)^{-1} +\lambda(z,\Theta)|G(\mathbf{x};\mathbf{x}_0;z)\rangle\langle G(\mathbf{x};\mathbf{x}_0;z)| , \tag{6}$$

with

$$\lambda(z,\Theta)=[1-\exp(i\Theta)]\left[(i-z)\int_\Omega G(\mathbf{x};\mathbf{x}_0,z)G(\mathbf{x};\mathbf{x}_0;i)d^2x+e^{i\Theta}(i+z)\int_\Omega G(\mathbf{x},\mathbf{x}_0,z)G(\mathbf{x},\mathbf{x}_0,-i)d^2x\right]^{-1} . \tag{7}$$

It is clear that the eigenvalues of the operator H_Θ coincide with the poles of the function $\lambda(z,\Theta)$. The poles of $\lambda(z,\Theta)$ are, however, given as zeros of the function

$$\Lambda(z,\Theta)=(i-z)\int_\Omega G(\mathbf{x};\mathbf{x}_0;z)G(\mathbf{x};\mathbf{x}_0;i)d^2x +e^{i\Theta}(i+z)\int_\Omega G(\mathbf{x};\mathbf{x}_0;z)G(\mathbf{x};\mathbf{x}_0;-i)d^2x . \tag{8}$$

Let us denote by $E_{n,m}$ the eigenvalues of the unperturbed Hamiltonian H,

$$E_{n,m}=n^2+a^2m^2 , \quad n,m=1,2,\ldots \tag{9}$$

and by $f_{n,m}$ the corresponding eigenvectors

$$f_{n,m}(x,y)=\frac{2\sqrt{a}}{\pi}\sin(max)\sin(ny)\ . \tag{10}$$

Using the resolvent identity

$$(H-z_1)^{-1}-(H-z_2)^{-1}=(z_1-z_2)(H-z_1)^{-1}(H-z_2)^{-1}\ , \tag{11}$$

and the expansion of the Green's function through the eigenfunctions and eigenvalues of the operator H,

$$G(\mathbf{x};\mathbf{y};z)=\sum_{n,m}\frac{f_{n,m}(\mathbf{x})f_{n,m}(\mathbf{y})}{E_{n,m}-z}\ , \tag{12}$$

we obtain for $\lambda(\Theta,z)$,

$$\lambda(\Theta,z)=(e^{i\Theta}-1)\sum_{n,m}[f_{n.m}(\mathbf{x}_0)]^2\left[\frac{1}{E_{n,m}-z}-\frac{E_{n,m}}{E_{n,m}^2+1}\right]-(e^{i\Theta}-1)\sum_{n,m}[f_{n,m}(\mathbf{x}_0)]^2\frac{\sin\Theta}{1-\cos\Theta}\left[\frac{1}{E_{n,m}^2+1}\right]\ . \tag{13}$$

Inserting this expansion back to the resolvent formula we finally get

$$(H_\Theta-z)^{-1}=(H-z)^{-1}-\frac{1}{\xi(z)-A(\Theta)}|G(\mathbf{x},\mathbf{x}_0,z)\rangle\langle G(\mathbf{x},\mathbf{x}_0,z)|\ , \tag{14}$$

with

$$\xi(z)=\sum_{n,m}|f_{n,m}(\mathbf{x}_0)|^2\left[\frac{1}{E_{n,m}-z}-\frac{E_{n,m}}{E_{n,m}^2+1}\right]\ , \tag{15}$$

and

$$A(\Theta)=\frac{\sin\Theta}{1-\cos\Theta}\sum_{n,m}|f_{n,m}(x_0)|^2\left[\frac{1}{E_{n,m}^2+1}\right]\ . \tag{16}$$

One can understand the operator H_Θ as a self-adjoint realization of the formal heuristic expansion

$$\tilde{H}_\mu=-\Delta+\mu(\Theta)\delta(\mathbf{x}-\mathbf{x}_0)\ , \tag{17}$$

with μ inversely proportional to $A(\Theta)$,

$$\mu=\frac{1}{A(\Theta)}\ . \tag{18}$$

Thus μ can be understood as the coupling constant of the point scatterer.

The levels of H_Θ are now obtained solving the transcendental equation

$$\xi(z)=\frac{1}{\mu}\ . \tag{19}$$

III. NUMERICAL STUDY OF THE BILLIARD

An investigation of the spectrum of chaotic systems usually requires quite complicated numerical work. In general one has to diagonalize large matrices to obtain the whole spectrum or to solve a large set of linear equations to get a single eigenvalue. The system discussed here offers an important virtue: each eigenvalue can be found numerically as a solution of the above-mentioned transcendental equation. Taking advantage of this fact we could easily obtain 20 000 eigenvalues, providing a sufficient sample for tests of the statistical properties of the spectrum.

We analyzed zeros of the meromorphic function $\xi(z)$ (15) corresponding to the rectangular billiard with $a=\pi/4$ (i.e., the sites of the billiard are of length π and 4.0), with the scattering point placed in the center: $\mathbf{x}_0=(2,\pi/2)$.

Considering only eigenstates with even-even parity we have taken the eigenvalues of the unperturbed system (9) of the form $E_{2n-1,2m-1}$, $m=1,\ldots,N$, $n=1,\ldots,N$, and ordered them according to the energy. Denoting this sequence by $\{E_j, j=1,\ldots,M\}$ one can rewrite Eq. (19) in the form

$$\frac{1}{\pi}\sum_{j=1}^{M}\left[\frac{1}{E_j-z}-\frac{E_j}{E_j^2+1}\right]-\frac{1}{\mu}=0\ . \tag{20}$$

This equation has precisely one solution between each pair of two neighboring poles of $\xi(z)$, which are given by eigenvalues E_j. According to Weyl's formula their mean spacing D is for this area of the billiard equal to 1; since we are interested in the states with even-even parity, the mean spacing between roots Z_j of Eq. (20) is equal to 4. Moreover, looking for a root of Eq. (20) localized between the poles E_l and E_{l+1} the summation can be cut to, say, $\sum_{j=l-500}^{j=l+500}$, so the numerical evaluating of the zero Z_l is straightforward.

Figure 2 presents the level-spacing distribution $P(s)$ for three values of the coupling constant μ. The histogram consists of 24 000 levels divided into 60 bins in each case. It is known [19] that for zero coupling constant the level statistics are well approximated by the Poisson distribution. Also for a small value of μ [$\mu=0.5$ in Fig. 2(a)] the data show a characteristic exponential decay for large values of spacing. Note, however, an interesting behavior of the distribution for small spacing. For $s\to 0$, the probability $P(s)\approx ks$ and linear level repulsion can be observed. Increasing the coupling constant μ to 1.0 [Fig. 2(b)] the slope k of the distribution decreases. The shape of histogram becomes closer to the Wigner distribution

$$P(s)=(s\pi/2)\exp(-s^2\pi/4)\ , \tag{21}$$

which is denoted by the dashed lines. However, even for infinite coupling constant [Fig. 2(c)] the resulting distri-

bution differs significantly from the Wigner surmise. The slope k is for small spacing larger than the value 1.645 predicted by the theory of random matrices [20,21]. On the other hand, the tail of the distribution decreases much more slowly when compared with results of the Gaussian orthogonal ensemble (GOE).

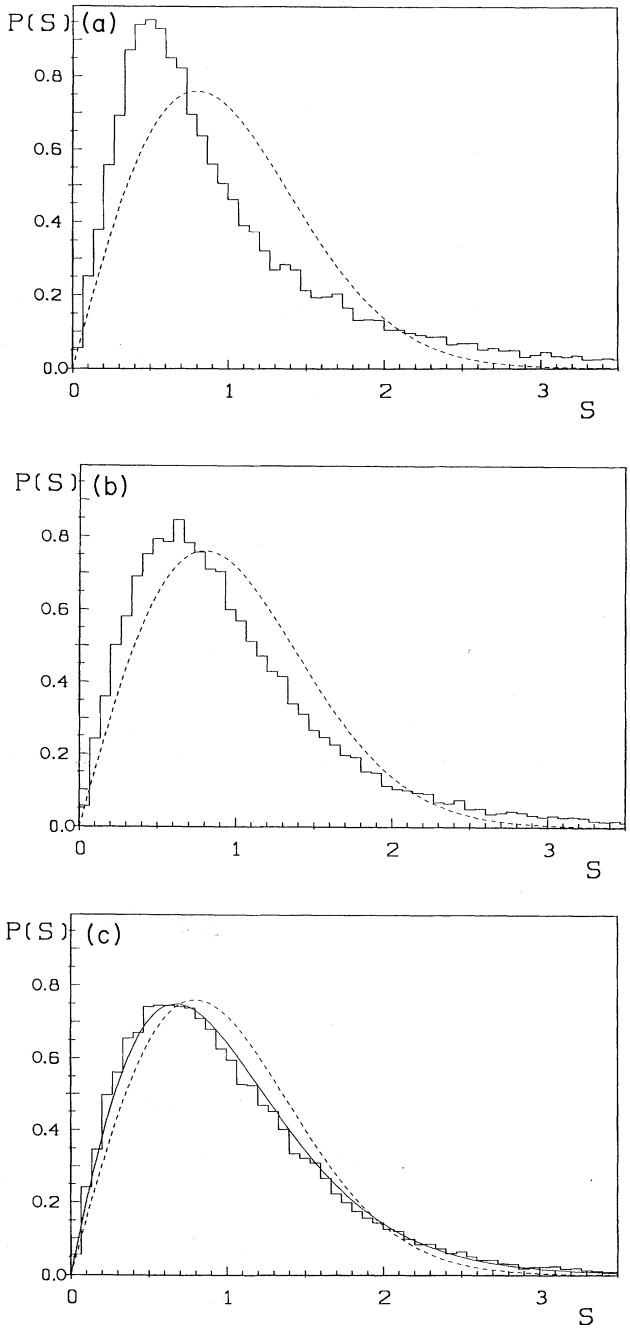

FIG. 2. Level-spacing distribution $P(s)$ for the rectangular billiard with the point scatterer placed in the center. Histograms contains 24 000 levels for three different values of the coupling constant (a) $\mu=0.5$, (b) $\mu=1.0$, (c) $\mu=\infty$. The dashed line represents the Wigner surmise; the solid line denotes the distribution (25).

The shape of the level-spacing statistics does not depend on the energy: the histogram made of the first 4000 levels of the billiard does not differ from the other one obtained taking levels belonging to the interval (20 000, 24 000).

A relatively good approximation of the considered distribution is provided by a simple heuristic calculation in the spirit of Wigner [22]. Given a level at E, let the probability that the next level be in $(E+s, E+s+ds), s \geq 0$ be $P(s)ds$. Let $r(s)$ denote the probability that interval of length s contains no levels and $T(s)ds$ in the conditional probability of finding exactly one level in the interval $(s, s+ds)$, provided that the interval $(0,s)$ contains no levels. The level-spacing distribution $P(s)$ is equal to

$$P(s)=r(s)T(s) \ . \tag{22}$$

Following the arguments of Wigner, we get for $P(s)$

$$P(s)=CT(s)\exp\left[-\int_0^s T(x)dx\right] . \tag{23}$$

In our case the eigenvalues are given by the roots of the meromorphic function (15), the poles of which have a Poisson distribution. One can therefore estimate the conditional probability $T(s)$ by

$$T(s)=Ase^{-Bs} , \tag{24}$$

with A and B constants. Inserting this expression into (23) we get

$$P(s)=As\exp\left[-Bs-\frac{A}{B^2}[1-e^{-Bs}(bs+1)]\right] , \tag{25}$$

which is represented by a solid line in Fig. 2(c). The constants A and B are determined by the normalized conditions

$$\int P(s)ds=1 , \tag{26}$$

$$\int sP(s)ds=1 , \tag{27}$$

which leads to $A\approx 2.1266$, $B\approx 0.3481$.

Recently it has been rigorously proved [23] that the slope k of the distribution obeys $1\leq k\leq \frac{9}{4}$. For large s values the following estimate holds $P(s)\geq se^{-s}$, in contradiction to the e^{-s^2} behavior characteristic for the GOE distribution. The level-spacing distribution obtained by numerical computations seems to fulfill both these requirements.

In order to analyze the long-range correlation of the spectrum, the number variance [24] Σ_2 was calculated. Figure 3 presents the dependence of Σ_2 on L for the case of infinite coupling ($\mu=\infty$). For small values of L the variance grows linearly, but the slope is much smaller than in the Poissonian case, denoted in the picture by a dashed straight line. For larger values of L ($L>15$) the curve saturates, as was already reported for several other systems [25]. Long-range statistical properties of our system are thus quite different from the prediction of the GOE, which is represented by the narrow solid line.

The self-adjoint-extensions approach described in Sec. II also provides information on the eigenfunctions Ψ_j.

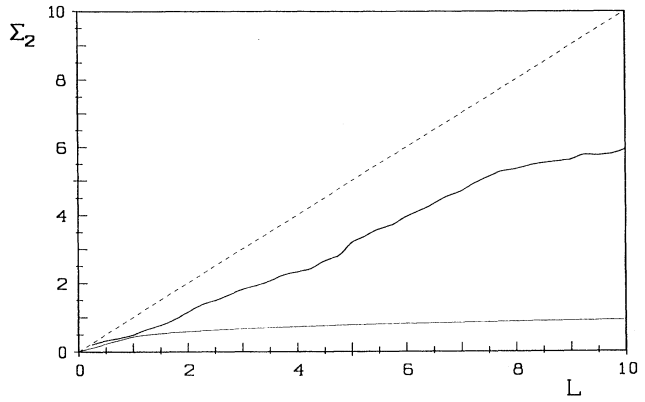

FIG. 3. Number variance $\Sigma_2(L)$ for the perturbed billiard with $\mu=\infty$. The solid line represents the GOE prediction; the dashed line shows the results for the Poisson spectrum.

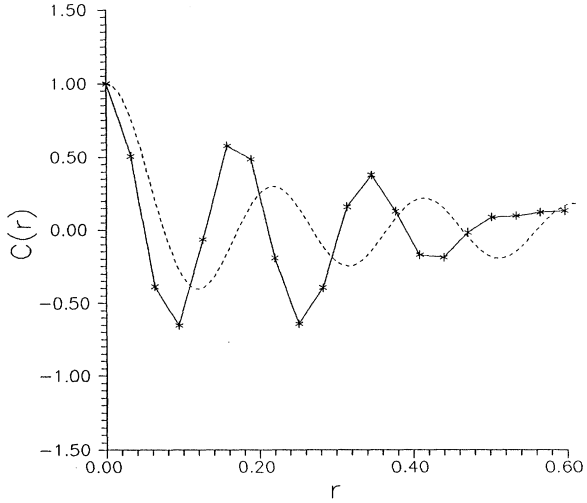

FIG. 5. Spatial correlation calculated for the 1000th eigenstate. The dashed line is the J_0 correlation valid for quantized chaotic billiards.

Analyzing the residual of the corresponding pole of the resolvent (14), one gets

$$\Psi_j(\mathbf{x})=\sum_{j=1}^{M}\frac{f_j(\mathbf{x})f_j(\mathbf{x}_0)}{E_j-Z_j}\ . \tag{28}$$

The eigenfunctions $f_j(\mathbf{x})$ of the unperturbed rectangular billiard are simple harmonic waves, so the above equation directly gives the two-dimensional Fourier expansion of the investigated function $\Psi_j(\mathbf{x})$. The eigenfunction displays quite irregular structure—see Fig. 4. It has been shown in the previous work [15] that $\Psi(\mathbf{x})$ behaves like a Gaussian random variable. This coincides with the GOE predictions. The other features of Ψ, like, for instance, the spatial correlation $C(\mathbf{x},\mathbf{r})=\langle\Psi(\mathbf{x}+\frac{1}{2}\mathbf{r})\Psi^*(\mathbf{x}-\frac{1}{2}\mathbf{r})\rangle$ (where $\langle\ \rangle$ denotes the local average) are however, expected to behave differently than those of the typical

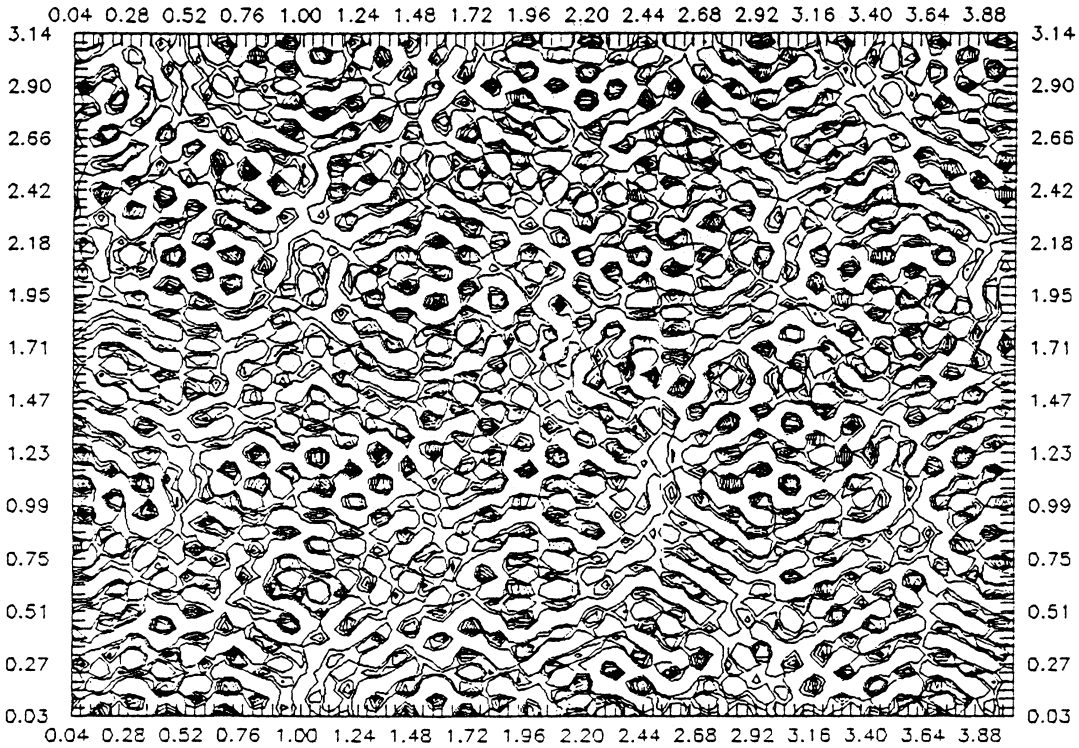

FIG. 4. Contour plot of the wave function corresponding to the 2600th state. In order to avoid the symmetry we localized the scatterer, not in the center but in the point $(4/\pi,1)$. The wave function has been calculated using the formula (28).

quantum chaotic billiard. In systems with a classically chaotic counterpart a single trajectory covers the whole energy surface in phase space. One can therefore expect that the Wigner function

$$W(\mathbf{x},\mathbf{k})=\int_{-\infty}^{\infty}\Psi(\mathbf{x}+\tfrac{1}{2}\mathbf{r})\Psi^*(\mathbf{x}-\tfrac{1}{2}\mathbf{r})e^{-i\mathbf{k}\cdot\mathbf{r}}d^n r \tag{29}$$

(which represents the phase-space distribution of the quantum state Ψ) behaves similarly. The most simple approximation of W is then [26]

$$\langle W(\mathbf{x},\mathbf{k})\rangle \approx \delta(H(\mathbf{x},\mathbf{k})-E_n)\ , \tag{30}$$

where H is the classical Hamiltonian and E_n is the eigenvalue corresponding to Ψ. In the case of the chaotic billiard this approximation leads to spatial correlation given by [27]

$$C(\mathbf{x},\mathbf{r})=J_0(\sqrt{E_n}r)\ , \tag{31}$$

where J_0 stands for the ordinary Bessel function. This type of behavior has been found numerically by McDonald and Kaufman in the Bunimovich stadium [28].

In the case of wave-chaotic systems we have to deal with a completely different situation. The phase-space trajectories do not fill the whole energy surface uniformly and are usually confined to some invariant manifold of higher genus—see [29]. Hence the above scenario does not apply and the spatial correlation of the wave function in such systems may differ from (31). The spatial correlation calculated for the 1000th energy eigenstate of the perturbed billiard is plotted on Fig. 5. The difference from the dashed curve representing Eq. (31) is significant indeed.

Some eigenfunctions of quantum chaotic systems exhibit specific regular structures, called quantum scars [6,30], which can be associated with the classical periodic orbits. Similar structures do exist also in the wave-chaotic case. Typical examples of such eigenstates are shown in Fig. 6. The corresponding periodic orbits can be recognized immediately.

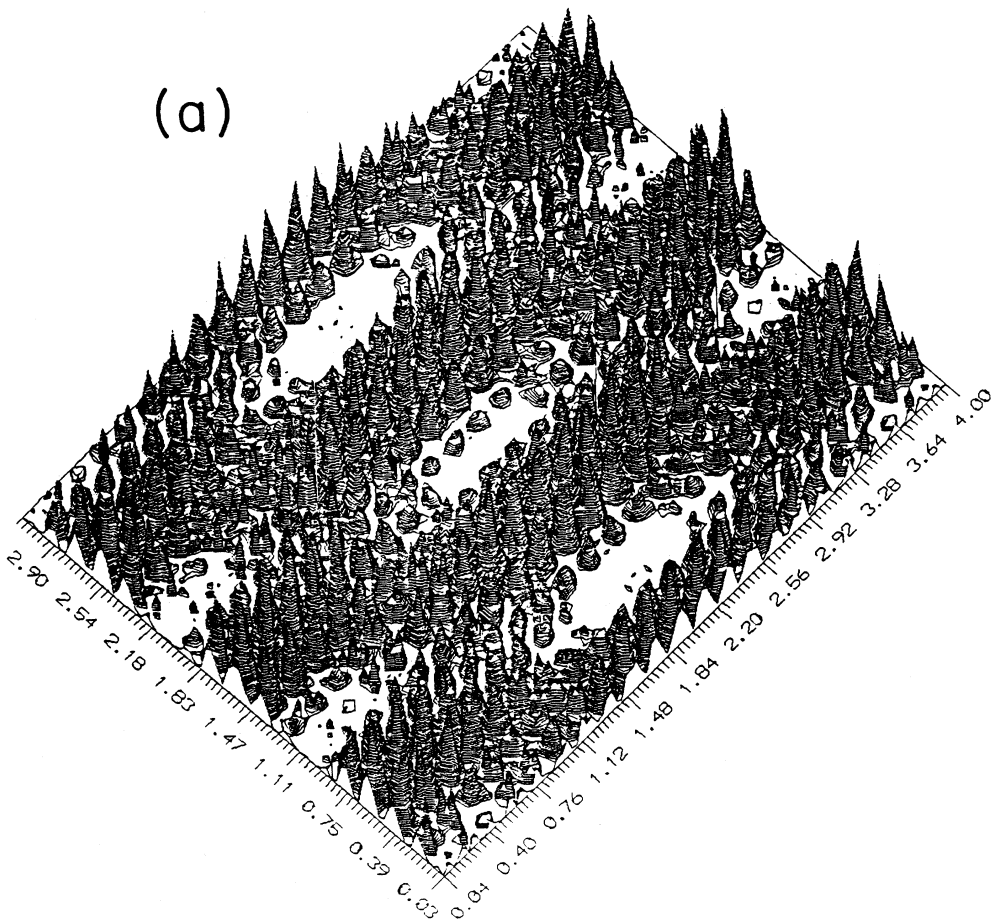

FIG. 6. Contour plot of the scarred wave functions: (a) scatterer in the center; (b) scatterer at the same point as in Fig. 4.

IV. DISTRIBUTION OF ZEROS OF A MEROMORPHIC FUNCTION

The analysis of the rectangular billiard with a point perturbation corresponds to the following general problem: what is the spacing distribution of zeros of a meromorphic function for a given distribution of poles?

As was shown in the 1950s by Wigner [31], there is a wide class of distributions that are invariant under such transformations. For example, if the statistics of the poles are given by the Wigner surmise (21), then the roots of meromorphic function are distributed according to the same distribution (we have checked this fact numerically with high accuracy). In connection with the system analyzed in this paper, this fact has interesting physical consequences; namely, the addition of the point scatterer into a system that is already chaotic [i.e., the poles of the function (16) have a Wigner distribution] does not change its level-spacing statistics.

Our aim is to investigate the influence of the pole statistics on the statistics of zeros in more detail. Let us therefore consider the following function:

$$\zeta(z)=\sum_{j=1}^{\infty} p_j \left[\frac{1}{E_j - z} - \frac{E_j}{E_j^2+1} \right], \tag{32}$$

where the poles E_j fulfill $E_{j+1}>E_j$, and their spacings $t_j=E_{j+1}-E_j$ are distributed according to a given distribution $P_1(t)$. For convenience we can assume that the mean spacing $\langle t \rangle$ is equal to 1. We are interested in the statistics of spacings s between subsequent roots Z_j of the equation $\zeta(z)=0$. Since it seems hardly possible to find the answer analytically we shall restrict ourselves to a numerical experiments.

For the pole statistics $P_1(t)$ we used the Berry-Robnik distribution

$$P_b(t)=(1-b)^2 e^{-t(1-b)}\mathrm{erfc}[\sqrt{(\pi)}bt/2] + 2[b(1-b)+\pi b^3 t/2]e^{-t(1-b)-\pi b^2 t^2/4}, \tag{33}$$

where $\mathrm{erfc}(x)=2(\pi)^{-1/2}\int_x^{\infty} t\, e^{-t^2}$ is the error function and b is a free parameter ranging from 0 to 1. This distribution was introduced in [32] to describe the behavior of quantum systems, the classical analog of which are only

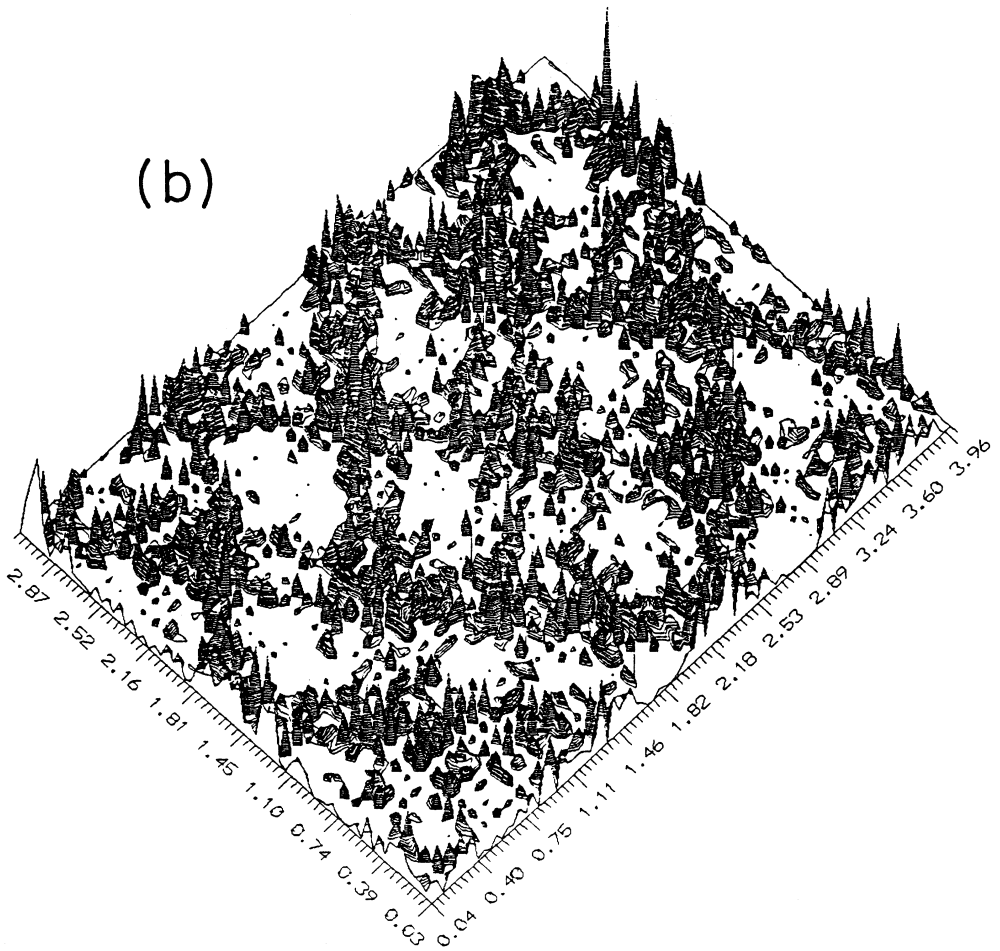

FIG. 6. (*Continued*).

partially chaotic, i.e., the corresponding phase space is only partially occupied (with fraction b) by the chaotic layer. In the limiting cases one obtains the Poisson distribution for $b=0$ and the Wigner distribution for $b=1$.

The above choice of pole statistics is motivated by a simple physical system: a rectangular billiard in a perpendicular constant magnetic field [33]. This system has a classical stochastic layer, the thickness of which depends on the intensity of the field applied. The statistics of the poles in our experiment corresponds to the distribution of the eigenvalues of the unperturbed system and hence the choice (33) seems to be reasonable. The roots then determine the eigenvalue statistics of the billiard in the magnetic field perturbed additionally by a point scatterer.

In order to mimic this physical system more closely we need some assumptions, concerning the coefficients p_j in (32). We choose

$$p_j=(C+\eta_j)^2 , \tag{34}$$

where C is a constant and η_j is a Gaussian random variable with distribution $P(\eta)=(2\pi\sigma^2)^{-1/2}\exp(-\eta^2/2\sigma^2)$. According to (15) the coefficients p_i describe the squared modulus of the jth eigenfunction in the scattering point $\mathbf{x}_0$. Having in mind the classical phase-space structure of the systems one can consider the wave function Ψ as a superposition of the "regular" part represented by a constant, and a "chaotic" part represented by the Gaussian random variable. The assumption $\langle t \rangle=1$ is equivalent to setting the billiard's area D to 4π. The normalization condition $\int_D|\Psi|^2 d\Omega=1$ provides a relation between the two terms: $c^2+\sigma^2=1/4\pi$. The relative weight remains as a free parameter.

We shall consider the two following cases.

Case (i),

$$C^2=\frac{1-b+\alpha b}{4\pi} , \quad \sigma^2=\frac{b(1-\alpha)}{4\pi} . \tag{35}$$

Case (ii),

$$C^2=\frac{(1-b)(1-\alpha)}{4\pi} , \quad \sigma^2=\frac{b+\alpha(1-b)}{4\pi} . \tag{36}$$

Case (i) describes the situation where the scattering point is localized in the classical island of stability; case (ii) represents the other possibility of point perturbation placed in the chaotic part of the phase space. The parameter b of the Berry-Robnik distribution is determined by the thickness of the chaotic layer, while the other parameter α (referred to as localization parameter) is taken to be $0\le\alpha\le1$. In the limiting case of $\alpha=1$ the "chaotic" wave function is localized completely in the classically chaotic region of the phase space b. For $\alpha<1$ the wave function can tunnel between the chaotic and the nonchaotic part of phase space. In the same way, the chaotic part of the wave function also contributes in the case with the point interaction localized in the classically nonchaotic region and vice versa. The other limiting case, $\alpha=0$, describes the completely delocalized regime where cases (i) and (ii) are equivalent.

To study the statistics of the roots of the function (32) the coefficients $\{p_j, j=1,\ldots,M\}$ and poles $\{E_j, j=1,\ldots,M\}$ were produced with the help of a random-number generator. The Berry-Robnik distribution $P_b(t)$ was obtained by overlapping two sequences of numbers with Wigner and Poisson distributions. The mean level spacing of these sequences was equal to $1/b$ and $1/(1-b)$, respectively.

Figure 7 presents histograms consisting of 29 500 roots

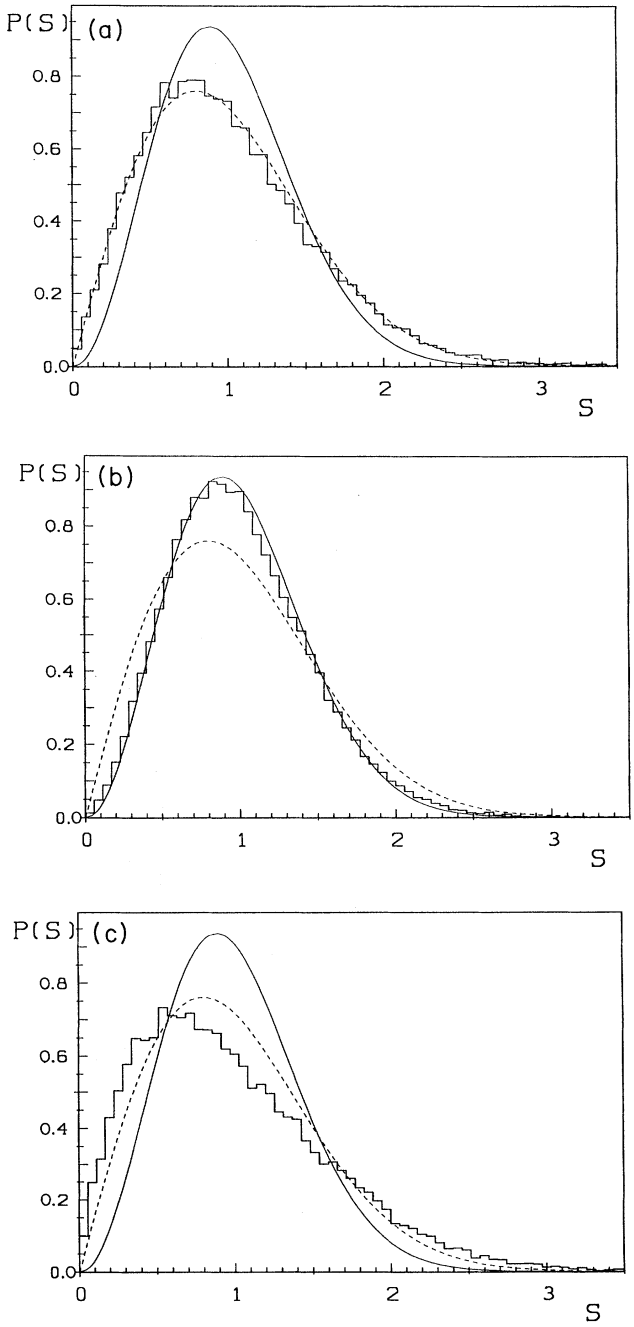

FIG. 7. Statistics of roots of the meromorphic function with poles distributed according to the Berry-Robnik formula: (a) $b=0.5$; (b) and (c) $b=0.9$ with different assumptions for the coefficient statistics. The dashed line represents the GOE and solid line for the GUE distributions.

each, for $\alpha=0.8$ and different values of b. For $b=0$ one confronts the Poisson pole distribution and the result coincides with the distribution considered in Sec. III. For the case of $b=0.5$ presented in Fig. 7(a) the root statistic coincides with the prediction of the GOE. On the other hand, the statistics of the Gaussian unitary ensemble (GUE),

$$P(s)=\frac{32s^2}{\pi^2}e^{-4s^2/\pi}, \tag{37}$$

seems to be appropriate for the histogram presented in Fig. 7(b) and obtained for $b=0.9$. This class of random matrices describes systems without antiunitary symmetry [34]. In our computation it might correspond to the physical case, where the magnetic field breaks the time-reversal symmetry, and the scattering point breaks the additive space symmetry of the system. These two cases were produced under condition (35) for the scattering point in the "regular" part of our fictitious billiard. Figure 7(c) shows results for $b=0.9$ with conditions (36): the histogram is now closer to the predictions of the orthogonal ensemble. The statistics of roots of the meromorphic function depends thus strongly on the statistics of the poles as well as on statistics of the weight coefficients.

V. CONCLUDING REMARKS

The quantum rectangular billiard with point scatterer is a model that displays typical wave-chaotic behavior. The numerical as well as theoretical studies have shown that its eigenvalue statistics do not conform to the prediction of the GOE, which is used to describe the behavior of the quantum chaotic systems. This model is a simple example of a system that has a set of classical unstable trajectories of measure zero. We speculate that similar behavior is present also in other quantum systems whose classical counterparts have the same property (pseudointegrable systems). If this speculation proves to be true, we have to do with a new phenomenon—wave chaos—in which the quantization procedure induces chaotic properties in systems that are classically nonchaotic. The recent numerical results of [35] seem to support this point of view. (See also [36] for the quantization of the rhomboidal billiard.)

ACKNOWLEDGMENTS

It is a pleasure to thank Fritz Haake for encouragement and helpful remarks. We have also benefitted from fruitful discussions with Michael Berry, Felix Izrailev, Marek Kuś and Akira Shudo. Financial support by the Alexander von Humboldt Stiftung and Sonderforschungsbereich 237 of the Deutsche Forschungsgemeinschaft is gratefully acknowledged.

*On leave from the Institute of Nuclear Physics, Czechoslovak Academy of Sciences, Řež near Prague, Czechoslovakia, and the Joint Institute of Nuclear Research, Dubna, U.S.S.R.

†On leave from Istytut Fizyki, Uniwersytet Jagielloński, ul. Reymonta 4, 30-059 Kraków, Poland.

[1] M. V. Berry, Proc. R. Soc. London Ser. A **413**, 183 (1987).
[2] F. Haake, M. Kuś, and R. Scharf, Z. Phys. B **65**, 381 (1987).
[3] G. Casati, B. V. Chirikov, and D. L. Shepelyanski, Phys. Rep. **154**, 79 (1987).
[4] B. Eckhardt, Phys. Rep. **163**, 207 (1988).
[5] J. Ford, in *Directions in Chaos,* edited by Hao Bai Lin (World Scientific, Singapore, 1988), Vol. II.
[6] E. J. Heller, Phys. Rev. Lett. **53**, 1515 (1984).
[7] A. Voros, Helv. Phys. Acta **62**, 595 (1989).
[8] G. Casati, I. Guarneri, F. Izrailev, and R. Scharf, Phys. Rev. Lett. **64**, 5 (1990).
[9] H. J. Stockmann and J. Stein, Phys. Rev. Lett. **64**, 2215 (1990).
[10] A. Shudo and T. Matsushita, Phys. Rev. A **41**, 1912 (1990).
[11] M. V. Berry, Proc. R. Soc. London Ser. A **400**, 229 (1985).
[12] Ya. G. Sinai, Russ. Math. Surv. **25**, 137 (1970).
[13] M. V. Berry, Ann. Phys. (Leipzig) **131**, 163 (1981).
[14] O. Bohigas, M. J. Giannoni, and C. Schmidt, Phys. Rev. Lett. **52**, 1 (1984).
[15] P. Šeba, Phys. Rev. Lett. **64**, 1855 (1990).
[16] J. P. Antoine, F. Gesztesy, and J. Shabani, J. Phys. A **20**, 3587 (1987).
[17] S. Albeverio, F. Gesztesy, R. Hoegh-Krohn, and H. Holden, *Solvable Models in Quantum Mechanics* (Springer-Verlag, Berlin, 1988).
[18] J. Zorbas, J. Math. Phys. **21**, 840 (1980).
[19] G. Casati, B. V. Chirikov, and I. Guarneri, Phys. Rev. Lett. **54**, 1350 (1985).
[20] M. L. Mehta, *Random Matrices* (Academic, New York, 1967).
[21] B. Dietz and F. Haake, Z. Phys. B **80**, 153 (1990).
[22] E. P. Wigner, Ann. Math. SIAM Rev. **9**, 1 (1967).
[23] S. Albeverio and P. Šeba (unpublished).
[24] M. V. Berry, Nonlinearity **1**, 399 (1988).
[25] M. V. Berry, Proc. R. Soc. London Ser. A **400**, 229 (1985).
[26] A. Voros and M. Berry, Ann. Inst. H. Poincaré A **24**, 31 (1976).
[27] M. V. Berry, J. Phys. A **10**, 2083 (1977).
[28] S. W. McDonald and A. N. Kaufman, Phys. Rev. A **37**, 3067 (1988).
[29] P. J. Richners and M. V. Berry, Physica D **2**, 495 (1981).
[30] M. V. Berry, Proc. R. Soc. London Ser. A **423**, 219 (1989).
[31] E. P. Wigner, Ann. Math. SIAM Rev. **9**, 1 (1967).
[32] M. V. Berry and M. Robnik, J. Phys. A **17**, 2413 (1984).
[33] M. Robnik and M. V. Berry, J. Phys. A **18**, 1361 (1985).
[34] F. Haake, *Quantum Signatures of Chaos* (Springer-Verlag, Berlin, in press).
[35] T. Cheon, T. Mizusaki, T. Shigehara, and N. Youshinaga (unpublished).
[36] D. Biswas and S. R. Jain, Phys. Rev. A **42**, 3170 (1990).